



Factors regulating primary producers' assemblages in *Posidonia oceanica* (L.) Delile ecosystems over the past 1800 years

Carmen Leiva-Dueñas^{a,*}, Peter R. Leavitt^{b,c}, Teresa Buchaca^a, Antonio Martínez Cortizas^{a,d}, Lourdes López-Merino^d, Oscar Serrano^e, Paul S. Lavery^{a,e}, Stefan Schouten^{f,g}, Miguel A. Mateo^{a,e}

^a Centro de Estudios Avanzados de Blanes, Consejo Superior de Investigaciones Científicas, Blanes, Spain

^b Institute of Environmental Change and Society, University of Regina, Regina, Canada

^c Institute for Global Food Security, Queen's University Belfast, Belfast, United Kingdom

^d EcoPast (G1-1553), Facultade de Biología, Universidade de Santiago de Compostela, Santiago de Compostela, Spain

^e School of Natural Sciences and Centre for Marine Ecosystems Research, Edith Cowan University, Joondalup, Australia

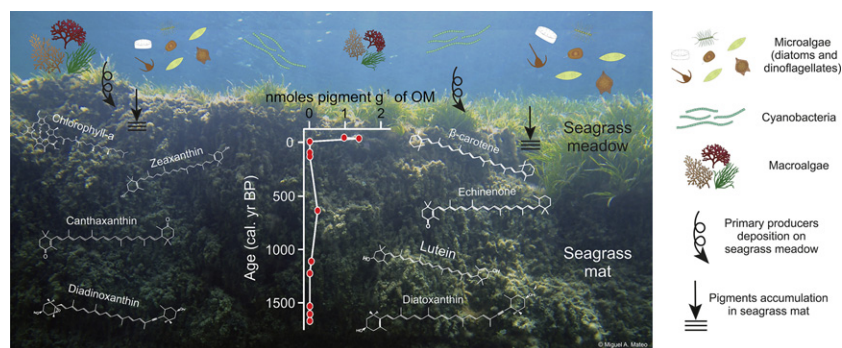
^f Department of Marine Biogeochemistry and Toxicology, Royal Netherlands Institute for Sea Research, Texel, the Netherlands

^g Department of Geosciences, Utrecht University, Utrecht, the Netherlands

HIGHLIGHTS

- Fossil pigments can be used to reconstruct seagrass phototrophic community.
- Phototrophic community composition was affected by local and global factors.
- Global climate factors explained long-term changes in the dinoflagellates abundance.
- Global warming may favour the development of dinoflagellates in seagrass meadows.
- Phototrophic community changes might impact the seagrass ecosystem functioning.

GRAPHICAL ABSTRACT



ARTICLE INFO

Article history:

Received 5 December 2019

Received in revised form 4 February 2020

Accepted 5 February 2020

Available online 6 February 2020

Editor: Lotfi Aleya

Keywords:

Late Holocene

Western Mediterranean

Seagrass

Primary producers' composition

Fossil pigments

Climate change

ABSTRACT

Posidonia oceanica (L.) Delile meadows are highly productive coastal marine ecosystems that provide multiple ecosystem services. The seagrass is not always the major contributor to total primary production, however, little is known about long-term changes in the composition of primary producers within seagrass meadows. Understanding compositional shifts within the community of primary producers is crucial to evaluate how climate and anthropogenic change affect the functioning of seagrass ecosystems. Here we analysed marker pigment composition in seagrass cores from two bays of the Cabrera Island (Balearic Islands, Spain) to assess long-term changes in phototrophic community composition and production in seagrass meadows, and identify the environmental factors triggering those changes. The proxy dataset was explored using principal component analyses (PCA): one including the pigment dataset to look for associations between producers' groups, and another one combining the pigment dataset with plausible local and global regulatory factors to assess the environmental drivers of change. Analyses of characteristic pigments and morphological fossils (cysts) showed that the abundance of dinoflagellates increased over the last 150–300 years, coeval with a rise in solar irradiance and air temperature. When compared among embayments, pigments from cyanobacteria predominated in seagrass meadows located at Es Port, a sheltered bay receiving higher terrestrial runoff; whereas pigments from diatoms, seagrasses and

* Corresponding author at: Centro de Estudios Avanzados de Blanes, Consejo Superior de Investigaciones Científicas, Carrer Accés Cala Sant Francesc, 14, 17300 Blanes, Spain.
E-mail address: cleiva@ceab.csic.es (C. Leiva-Dueñas).

rodophytes were more common at Santa Maria, an exposed bay with clearer waters. Water depth also played a role in controlling the phototrophic community composition, with greater abundance of diatoms in the shallowest waters (<5 m). Overall, our results suggested that historical and spatial variation in seagrass meadows' phototrophic community composition was influenced by the interaction between local factors (catchment-bay characteristics) and global climate processes (energy influx). Together these patterns forecast how marine primary producers and seagrass ecosystem structure may respond to future global warming.

© 2020 Elsevier B.V. All rights reserved.

1. Introduction

Posidonia oceanica seagrass meadows are one of the most valuable habitats in the Mediterranean Sea owing to their multiple ecosystem services (Spalding et al., 2003). However, this endemic species has exhibited widespread decline since the early 20th century, mainly due to local anthropogenic pressures such as coastal development, pollution, trawling, fish farming, moorings, dredging, dumping and introduced species (Boudouresque et al., 2009). Fortunately, de los Santos et al. (2019) showed that seagrass loss rates recently slowed down due to effective conservation and restoration actions, including habitat protection. Despite this promising news, relatively little is known about how *P. oceanica* meadows have varied historically in response to perturbations.

Therefore, elucidation of the long-term dynamics and environmental drivers of ecosystem change is required to evaluate the magnitude of current declines in an historical context, as well as to predict, prevent or mitigate the effects of present and future environmental changes on seagrass meadows structure and function (López-Merino et al., 2017; Leiva-Dueñas et al., 2018).

Total primary production of seagrass ecosystems does not always depend on the seagrass species as the major contributor. Other primary producers inhabiting the meadows can contribute substantially (up to 60% of total production), including epiphytes, phytoplankton, phytobenthos and macroalgae (McRoy and McMillan, 1977; Borowitzka et al., 2006; Mateo et al., 2006). The abundance and composition of primary producers' communities within seagrass meadows are regulated by complex mechanisms reflecting interactions between physico-chemical (e.g., light, temperature, water movement, nutrients) and biological factors (e.g., competition for space, grazing and predation) (Koch, 2001; Borowitzka et al., 2006) (Fig. 1). Regulation of composition at the decadal-scale appears to mainly

involve competition for light and nutrients between micro- and macroalgae and the seagrass (Delgado et al., 1999; Hemminga and Duarte, 2000; Ralph et al., 2006). Elevated nutrient concentrations favour phytoplankton blooms, as well as epiphyte and macroalgae overgrowth, all leading to attenuation of irradiance and diminished transmission to the seagrass canopy (McGlathery et al., 2007; Viaroli et al., 2008) (Fig. 1).

Epiphyte composition in seagrass leaves is influenced by complex interactions between nutrients, light, temperature, water motion, salinity, and seagrass physiological and phenological characteristics, as well as the biotic interactions between epiphytes, herbivores and predators (Armitage et al., 2006; Lavery et al., 2007; Prado et al., 2007; Mabrouk et al., 2014). In addition, epiphyte assemblages often vary predictably along a depth gradient due to changes in light, local hydrodynamics, and meadow structure (Borowitzka et al., 2006; Tsirika et al., 2007; Nesti et al., 2009; Piazzini et al., 2016) (Fig. 1).

Research on the factors regulating the complex interactions influencing coastal marine ecosystem production and composition over centennial timescales lags behind that of lacustrine and terrestrial habitats, mainly because of the relative scarcity of reliable coastal marine archives owing to their hydrodynamism (Hay, 1974; Mateo et al., 2010). *P. oceanica* meadows are an exception, since coherent sequences with high temporal resolution (2–17 yr cm⁻¹) can be obtained in them (Serrano et al., 2012; Serrano et al., 2016a). These *Posidonia* environmental archives, known as mats, consist of large pools of organic matter accumulated over millennia, mainly as decay-resistant plant debris and organic or inorganic remains of other meadow-inhabiting organisms (Mateo et al., 1997; Lo Iacono et al., 2008; Kaal et al., 2016). Therefore, mats can potentially preserve a wide range of biotic and abiotic

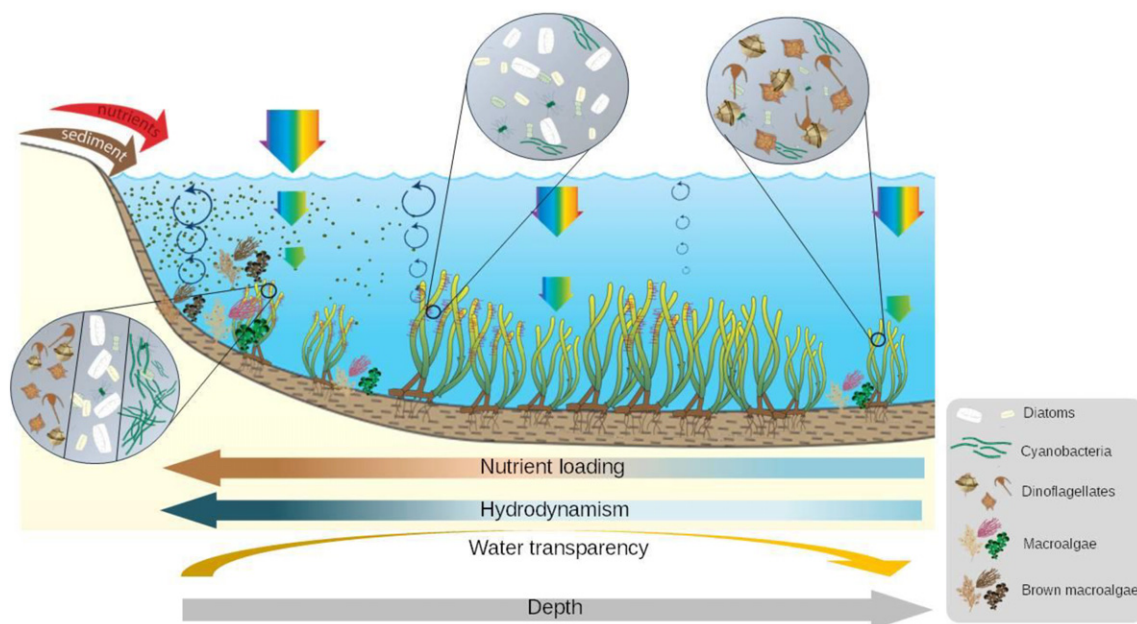


Fig. 1. Schematic diagram illustrating how nutrient and sediment inputs affect aquatic primary producers in seagrass meadows. Zooms are for micro-epiphytic community composition. Diagram made using image vectors from Image library in Integration and Application Network (ian.umces.edu).

proxies due to the prevailing anoxic conditions (Mateo et al., 2006; Piñeiro Juncal et al., 2018).

Proxy analyses on *Posidonia* mats allow quantification of diverse long-term environmental and ecological changes as, for example, the impact of land-use change and metal pollution on coastal systems, the role of climatic factors and seagrass revegetation in carbon burial, and historical variation in seagrass productivity (López-Sáez et al., 2009; Mateo et al., 2010; Serrano et al., 2011, 2013, 2016b, 2016c; Macreadie et al., 2015; Marba et al., 2015; López-Merino et al., 2015, 2017; Leiva-Dueñas et al., 2018). To date, however, fossils pigments from phototrophic organisms have not been used to quantify long-term changes in the production or gross community composition of seagrass systems, unlike studies on some other marine systems (Kowalewska et al., 2004; Rabalais et al., 2004; Reuss et al., 2005, 2010).

Aiming at filling the abovementioned knowledge gap, we measured past changes in concentrations of fossil pigments from diverse phototrophic organisms, in combination with other proxies (e.g., sedimentological, geochemical and dinoflagellate cysts), in five *P. oceanica* mat cores from two bays of the Cabrera National Park, Balearic Islands, Spain. The objectives of this study were: (1) to measure the variability in pigment composition through time and across spatial gradients (water depth within a bay) in two bays with contrasting features, and; (2) to identify the long-term environmental drivers which may regulate the phototrophic community composition in the meadows.

2. Material and methods

2.1. Environmental setting and coring procedures

The Cabrera Island is the largest island of the Cabrera Archipelago, located south of Mallorca (Balearic Islands) in the western Mediterranean Sea (Fig. 2). The climate of the island is semi-arid and although precipitation is scarce, there are several small watersheds that are active only during intense precipitation periods (Alcover et al., 1993). The main watershed drains into Es Port Bay (Rodríguez-Perea and Servera, 1993). The surrounding coastal waters are warm with very low nutrient content comparing to other coastal Mediterranean waters (Ballesteros and Zabala, 1993).

Five *P. oceanica* mat cores were taken in June 2015 from meadows growing in two bays: Santa Maria (SM), and Es Port (EP) (Fig. 2). Cores were collected at a single station 5-m below the sea level (bsl) at EP and along a depth-transect (5, 10, 15, and 25 m bsl) at SM (Table 1). SM is a relatively exposed bay with an area of 1.14 km² (55 m maximum depth) connected to the open sea by a 1.2-km wide mouth. On the contrary, EP (0.8 km², 45 m maximum depth) forms a relatively sheltered environment with a narrower opening (650 m) (Fig. 2). Cores were collected by scuba divers using high-density PVC pipes fitted with core catchers and a serrated leading edge. Exponential decompression functions were applied to correct for core shortening (Morton and White, 1997; Serrano et al., 2012).

At both bays, *P. oceanica* grows on biogenic, carbonate-rich and iron-deficient sediments (Holmer et al., 2005; Marbà et al., 2008). About 42%

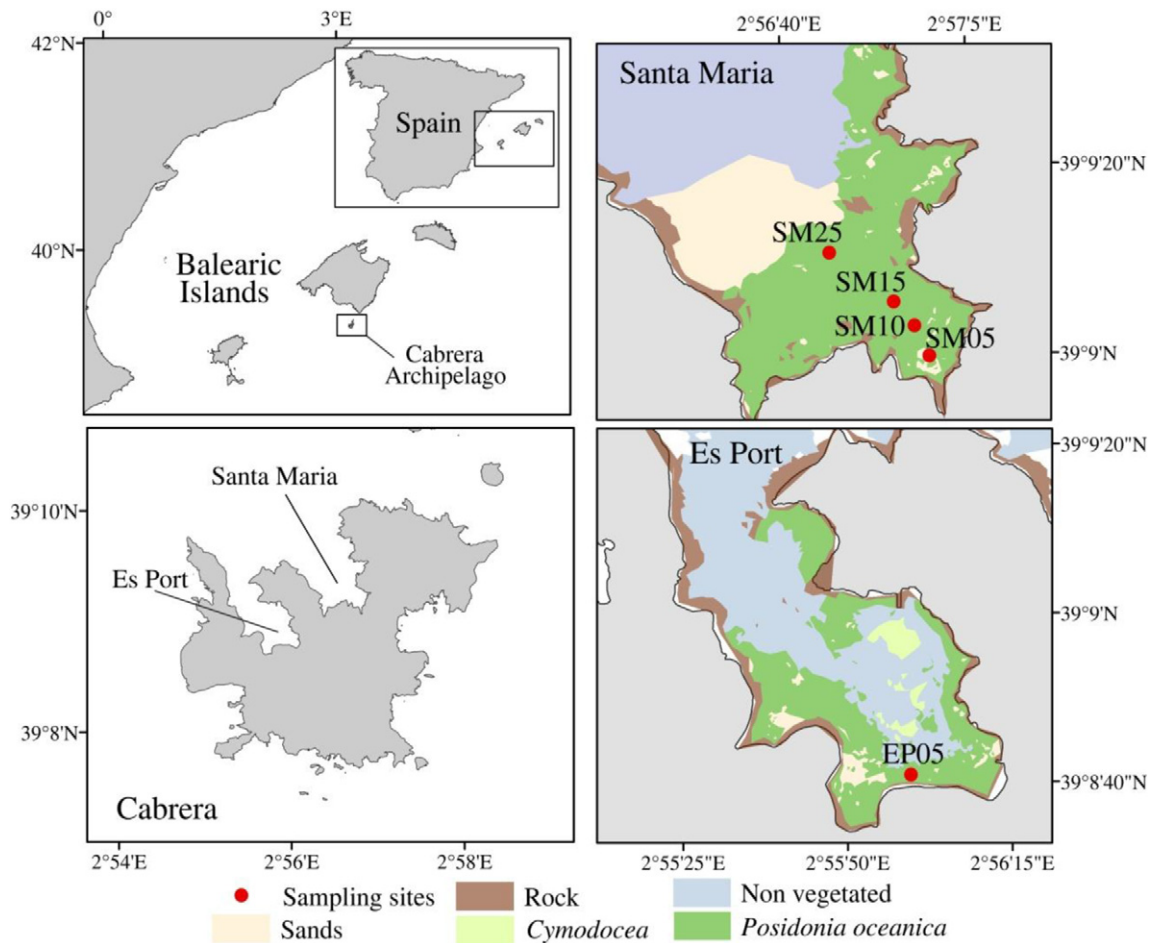


Fig. 2. Location of the Cabrera Archipelago as well as *P. oceanica* and *Cymodocea* meadows areal coverage in two bays: Santa Maria (SM) and Es Port (EP). Red dots indicate the core locations. The number stands for the sampling water depth (in meters below sea level).

Table 1
Details of the five cores taken from *Posidonia oceanica* meadows at two bays in the Cabrera Island (Balearic Islands, Spain).

| Core ID | Coordinates | | Sampling location | Water depth (m) | Compressed length (cm) | Decompressed length (cm) | Compression (%) |
|---------|-------------|-----------|-------------------|-----------------|------------------------|--------------------------|-----------------|
| SM05 | 39°9'0"N | 2°56'57"E | Santa María Bay | 5 | 49 | 83 | 42.4 |
| SM10 | 39°9'3"N | 2°56'55"E | Santa María Bay | 10 | 134 | 161 | 18.3 |
| SM15 | 39°9'6"N | 2°56'53"E | Santa María Bay | 15 | 113 | 138 | 19.3 |
| SM25 | 39°9'12"N | 2°56'44"E | Santa María Bay | 25 | 84 | 89 | 5.6 |
| EP05 | 39°8'42"N | 2°55'60"E | Es Port Bay | ~5 | 88 | 98 | 17 |

of SM benthos is covered by dense, continuous *P. oceanica* meadows, whereas meadows in EP cover less area (36%) and occur at shallower depth (Marbà et al., 2002). Demographic analysis indicates that while meadows at SM are in good condition, those at EP exhibit symptoms of stress, including lower leaf production rates and vertical rhizome elongation, very low shoot recruitment, higher mortality, and elevated sulphate reduction rates. The different seagrass conditions between bays have been attributed to contrasting water residence times in EP (7–15 days) and SM (4 days) (Marbà et al., 2002; Orfila et al., 1992, 2005), and to more frequent and intensive anthropogenic activities at EP (Marbà et al., 2002).

2.2. Sedimentology, geochemical analyses and core chronology

Cores were cut longitudinally and opened into two halves. One-half was analysed non-destructively for elemental composition using X-ray fluorescence (XRF) with an AVAATECH core scanner at the CORELAB laboratory, University of Barcelona. One cm-thick samples from one of the half-cores were dried at 60 °C until constant weight to determine dry bulk density, then homogenized using an automated agate mortar (Mortar Grinder RM-200 RETSCH).

Organic matter content (OM) was estimated in the samples by mass-loss-on-ignition at 550° for 4 h. Sediment grain size was determined using a laser-diffraction particle analyser (Mastersizer 2000, Malvern instruments Ltd., UK). Carbon and N elemental and isotopic composition of sediment samples were analysed at UH Hilo Analytical Laboratory, University of Hawaii at Hilo, on a Thermo-Finnegan Delta V IRMS isotope ratio mass spectrometer coupled with a Costech elemental analyser.

Isoprenoid glycerol dialkyl glycerol tetraether (GDGT) lipids were used to calculate the Branched and Isoprenoid Tetraether (BIT) index, an index of the relative abundance of terrestrial and autochthonous organic matter in marine sediments (Hopmans et al., 2004). The samples polar fraction were analysed for GDGTs according to Schouten et al. (2007). GDGT analyses were performed using liquid chromatography-mass spectrometry (LC-MS) with a Hewlett Packard1100 Series instrument equipped with an auto-injector and ChemStation chromatography manager software.

Radiocarbon (¹⁴C) and lead-210 (²¹⁰Pb) activities were measured using accelerator mass spectrometry (DirectAMS laboratory) and alpha spectrometry (Environmental Radioactivity Laboratory, Autonomous University of Barcelona), respectively, to obtain age-depth models for the collected cores.

Raw proxy data trends are presented in Fig. S1.

2.3. Fossil pigment analysis

Pigments and their derivatives were extracted, isolated, identified and quantified using high-performance liquid chromatography (HPLC) with an Agilent model 1100 instrument at University of Regina following standard methods of Leavitt and Hodgson (2001). Fossil pigment interpretations were restricted to a subset of carotenoid and chlorophyll biomarkers that commonly preserve in sedimentary deposits (Table 3). Predominant phorbins identified included metrics of total primary producers such as labile Chlorophyll-*a* (chl-*a*; a precursor), pheophytin *a* (Chl's stable product), and chlorophyte markers (chl-*b*,

pheophytin *b*). Pigment preservation index (PPI) was calculated from the ratio of chl-*a* to its degradation product pheophytin *a*. Complete fossil pigment profiles are presented in Fig. S2.

2.4. Organic-walled dinoflagellate cysts analysis

A palynological analysis of pollen and non-pollen palynomorphs (NPP) of the cores is currently under way. Among the NPP, we have identified organic-walled dinoflagellate cysts (dinocysts); microremains relevant for this study due to their relationship with some of the analysed pigments. The results from core EP05 and the preliminary results from core SM25 are presented herein. Pollen and NPP were isolated from seagrass deposits using standard palynological extraction protocols, including sediment digestion with HCl, NaOH and HF to eliminate carbonates, humic acids and silicates, respectively (Fægri and Iversen, 1989). Dinocysts were identified and counted using light microscopy at ×400 magnifications.

2.5. Numerical procedures

Principal component analysis (PCA) was used to explore potential associations in the community of primary producers as recorded by fossil pigment concentrations in the cores (PCA_{pigments}). Fossil pigment data were reported in units of concentration and, as such, are compositional data which required isometric log-ratio transformation prior the analysis (Aitchison, 1986; Egozcue et al., 2003; Filzmoser et al., 2010). The analysis consisted in a robust PCA via *pcaCoDa* command in “robcompositions” package in the R computational environment (Templ et al., 2011).

To determine which environmental variables were the most influential on pigment marker composition, another robust PCA was run including both local factors and global climate indicators (PCA_{environmental}). Local factors included biotic variables such as total primary production (as chl-*a*, β-carotene and OM), nutrient cycling and organic matter supply (C and N stable isotope values and BIT index), as well as abiotic descriptors (sediment grain size, and C and N elemental composition, XRF-measured elements). Global climate external factors included indices of Total Solar Irradiance (TSI, Vieira et al., 2011), Northern Hemisphere Temperature (NHT, Kobashi et al., 2013) and the North Atlantic Oscillation (NAO; Hurrell, 2003; Trouet et al., 2009; Olsen et al., 2012) - NAO is an atmospheric mode affecting the hydrological variability in the western Mediterranean (Roberts et al., 2012).

Generalized additive models (GAMs) were used to estimate temporal trends in the principal components scores and dinocyst concentrations. GAMs are able to model non-linear relationships between time and a response variable and can handle the irregular spacing typical in palaeoecological time series (Simpson, 2018). Thin-plate regression splines were used to parametrise the smooth functions of time (Wood, 2003). The differences between the fitted smooth functions for PC1_{pigments} scores and concentrations of dinocysts were calculated as in Rose et al. (2012). GAMs were performed using the mgcv package in R (Wood, 2004, 2017, Wood et al., 2016).

All statistical analyses were conducted using R statistical software (R Core Team, 2018) and detailed descriptions of the materials and methods section are given in Supplementary Material.

3. Results

3.1. Age-depth models

The age-depth models combining radiocarbon and ^{210}Pb dates revealed that core SM15 extended back to ~1900 cal. yr BP, whereas cores SM25 and EP05 extended to ~1700 cal. yr BP (Table 2, Fig. 3A). Cores SM05 and SM10 encompassed less time, SM05 dated back to ~100 and SM10 to ~700 cal. yr BP. Overall, accumulation rates varied between 0.02 and 2 cm/yr with significant differences among cores (median Kruskal-Wallis test, $p < 0.05$). A nonparametric pairwise multiple comparison (Dunn's test, $p < 0.05$) confirmed all median rates were significantly different with the exception of the pair EP05 - SM15 ($p = 0.754$). Accumulation rates decreased with increasing water depth in SM, from a median of 0.36 cm/yr (SM05) to a median of 0.06 cm/yr (SM25) (Fig. 3B). In most cores, mat accumulation was likely continuous with the exception of EP05 which exhibited an apparent hiatus between ~300 and ~1250 cal. yr BP - based on a large jump of ~950 calibrated years between two radiocarbon dates at 60 and 64 cm depth in the core (Fig. 3A and Table 2).

3.2. Primary producers' composition

Trends in the pigment composition within all cores were well described using a robust PCA with two principal axes, explaining 91% of the total variance (Fig. 4A). The first principal component ($\text{PC1}_{\text{pigments}}$, 78%) showed a high positive loading for diadinoxanthin (dinoflagellates, diatoms and chrysophytes) and moderate negative loadings for echinenone (total cyanobacteria), lutein-zeaxanthin (chlorophytes,

higher plants, rhodophytes and cyanobacteria) and canthaxanthin (Nostocales -cyanobacteria-) (Fig. 4A and Table 4). The second principal component ($\text{PC2}_{\text{pigments}}$, 13%) showed high positive loadings for diatoxanthin (mainly diatoms) and lutein-zeaxanthin (chlorophytes, higher plants, cyanobacteria and rhodophytes), and high-to-moderate negative loadings for echinenone (total cyanobacteria) and canthaxanthin (Nostocales -cyanobacteria-) (Fig. 4A and Table 5).

The main temporal trend observed in all cores was an increase in $\text{PC1}_{\text{pigments}}$ scores towards the present, particularly during the last ~150–300 years. This trend mainly reflects increasing concentrations of diadinoxanthin (Fig. 4B). Sample scores from $\text{PC2}_{\text{pigments}}$ did not show a consistent change through time, although they did show an evident spatial pattern, with different pigment composition between bays (Fig. 4). Higher proportions of diatoxanthin and lutein-zeaxanthin were found in SM, while canthaxanthin and echinenone predominated in EP. Within SM, sample scores indicated a greater abundance of diatoxanthin and lutein-zeaxanthin in the shallowest area (SM05) of the bay (Fig. 4B).

3.3. Relationship between fossil pigment composition and environmental factors

A robust PCA explained 57% of the variance in fossil pigment composition using a combination of local and global predictive variables (Fig. 5A and Table 5). The first axis ($\text{PC1}_{\text{environmental}}$) accounted for 31% of the total variance and showed that diadinoxanthin was strongly and positively correlated with global climate indicators (TSI and NHT). Diadinoxanthin content was also moderately and positively correlated to $\delta^{13}\text{C}$, concentrations of chl-*a*, and the PPI. Echinenone and lutein-

Table 2

Radiocarbon dates in the *P. oceanica* mat cores retrieved at the Cabrera Island. The marine ^{14}C calibration curve (Reimer et al., 2013) was used for calibration of the radiocarbon dates together with a local marine reservoir effect (mean \pm SD; $\Delta R = 26 \pm 24$ years; Riera Rullan, 2016).

| Core | Laboratory code | Decompressed depth (cm) | AMS ^{14}C date (yr BP) | | Cal. yr BP (2 σ range) | | | Weighted mean age |
|------|-----------------|-------------------------|----------------------------------|----------|-------------------------------|---|------|-------------------|
| EP05 | D-AMS 014002 | 32 | 398 | \pm 23 | 58.5 | – | 92.4 | 75.8 |
| | D-AMS 019447 | 34 | 379 | \pm 24 | 66.7 | – | 108 | 87.1 |
| | D-AMS 014003 | 43 | 467 | \pm 27 | 104 | – | 190 | 141.3 |
| | D-AMS 012768 | 54 | 502 | \pm 27 | 166 | – | 277 | 215.4 |
| | D-AMS 029626 | 60 | 545 | \pm 30 | 202 | – | 349 | 263.6 |
| | D-AMS 019448 | 64 | 1741 | \pm 28 | 1185 | – | 1531 | 1369 |
| | D-AMS 012769 | 75 | 1940 | \pm 26 | 1305 | – | 1620 | 1468.9 |
| | D-AMS 012770 | 96 | 1788 | \pm 29 | 1473 | – | 1473 | 1651.6 |
| SM05 | D-AMS 012771 | 57 | 75 | \pm 26 | 18.8 | – | 51.1 | 33.9 |
| | D-AMS 012772 | 68 | 105 | \pm 28 | 43.2 | – | 87.4 | 64.6 |
| | D-AMS 013117 | 78 | 366 | \pm 25 | 66.5 | – | 120 | 92.9 |
| | D-AMS 012773 | 79 | 439 | \pm 25 | 69.1 | – | 122 | 95.7 |
| SM10 | D-AMS 019434 | 34 | 104 | \pm 25 | –0.9 | – | 7.2 | 3.2 |
| | D-AMS 019436 | 58 | 449 | \pm 28 | 83.9 | – | 163 | 117.6 |
| | D-AMS 019437 | 63 | 384 | \pm 29 | 103 | – | 138 | 141.1 |
| | D-AMS 019438 | 70 | 479 | \pm 26 | 130 | – | 228 | 177.1 |
| | D-AMS 022098 | 88 | 593 | \pm 61 | 225 | – | 334 | 275.2 |
| | D-AMS 022099 | 110 | 740 | \pm 34 | 348 | – | 462 | 405.6 |
| | D-AMS 022100 | 124 | 970 | \pm 45 | 434 | – | 551 | 494.6 |
| | D-AMS 022102 | 152 | 1063 | \pm 43 | 588 | – | 740 | 657.5 |
| SM15 | D-AMS 019444 | 50 | 610 | \pm 24 | 89.4 | – | 242 | 151.8 |
| | D-AMS 012774 | 55 | 573 | \pm 23 | 126 | – | 305 | 207.6 |
| | UBA-32342 | 75 | 1732 | \pm 32 | 752 | – | 1154 | 996.7 |
| | D-AMS 019445 | 78 | 1508 | \pm 29 | 899 | – | 1169 | 1044.9 |
| | D-AMS 012775 | 89 | 1583 | \pm 23 | 1058 | – | 1269 | 1163.3 |
| | D-AMS 012776 | 104 | 2447 | \pm 32 | 1269 | – | 1703 | 1477.9 |
| | D-AMS 029627 | 120 | 2106 | \pm 29 | 1482 | – | 1845 | 1664.7 |
| | D-AMS 029628 | 135 | 1556 | \pm 29 | 1634 | – | 2098 | 1830.1 |
| SM25 | D-AMS 019439 | 8 | 216 | \pm 46 | –49.5 | – | 63.9 | 7.3 |
| | D-AMS 014000 | 28 | 508 | \pm 20 | 76.7 | – | 243 | 165.3 |
| | D-AMS 019440 | 35 | 608 | \pm 27 | 144 | – | 303 | 229.2 |
| | D-AMS 014001 | 39 | 604 | \pm 29 | 181 | – | 383 | 271.8 |
| | D-AMS 012777 | 49 | 1000 | \pm 27 | 427 | – | 637 | 537.7 |
| | D-AMS 019441 | 56 | 1234 | \pm 27 | 628 | – | 852 | 728 |
| | D-AMS 012778 | 70 | 1957 | \pm 24 | 1170 | – | 1525 | 1374.6 |
| | D-AMS 019442 | 76 | 1985 | \pm 25 | 1428 | – | 1533 | 1532.2 |
| | D-AMS 012779 | 89 | 2178 | \pm 28 | 1619 | – | 1871 | 1748.5 |

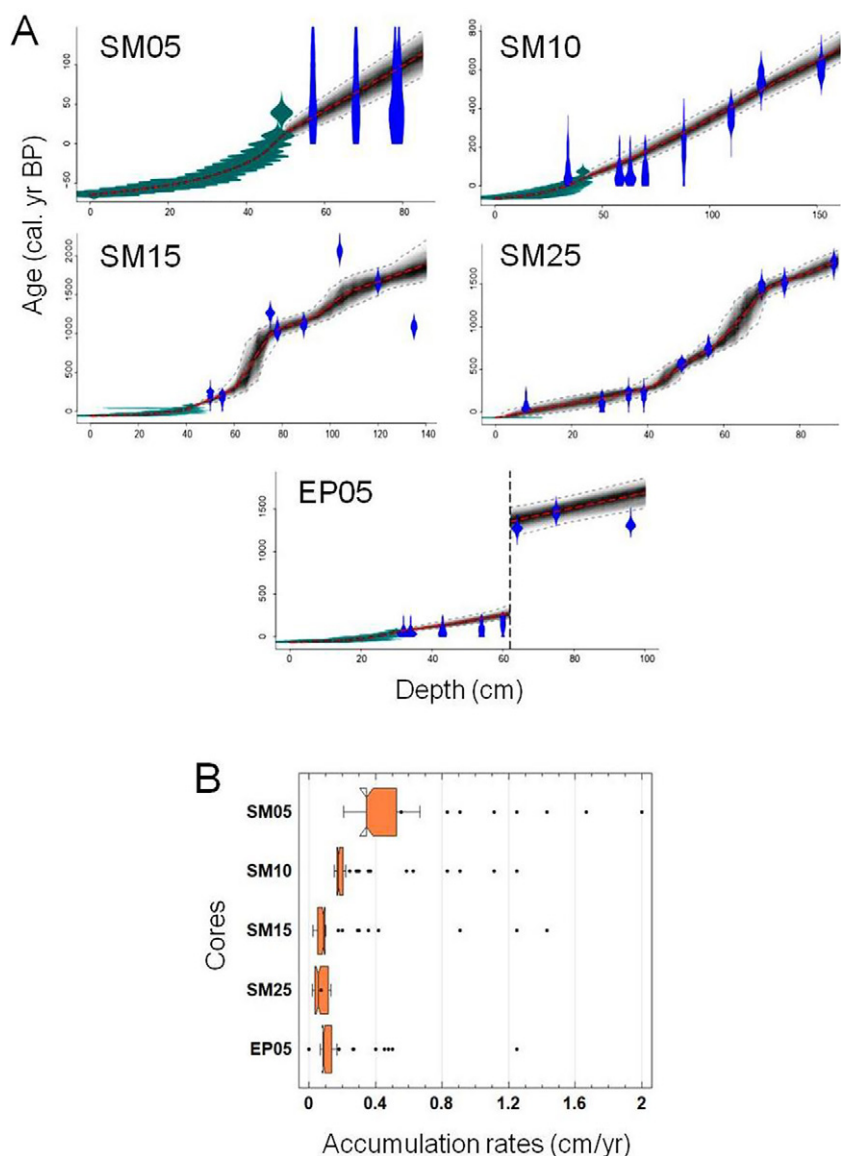


Fig. 3. A) Bayesian age depth-models of Cabrera Island cores using Bacon. R software (Blaauw & Christen, 2011). Lead-210 (in green) and radiocarbon (in blue) dates were included in the age-depth models. Radiocarbon dates were calibrated using the *marine 13* calibration curve (Reimer et al., 2013) and corrected for a local marine reservoir effect (mean \pm SD; $\Delta R = 26 \pm 24$ years; Riera Rullan, 2016). The red dashed curve shows the “best” model based on the weighted mean age for each depth. Individual radiocarbon dates are shown in probability density functions of calibrated ages. The grey area indicates the uncertainty envelope of the model with grey dashed curves indicating 95% confidence intervals. The vertical, dashed black line on the EP05 model denotes a hiatus. B) Notched box-plot of accumulation rates for each of the sampled cores.

zeaxanthin abundances were also correlated moderately and negatively with diadinoxanthin (Fig. 5A).

PC2_{environmental} accounted for 26% of the total variation (Fig. 5A). On this axis, abundances of diatoxanthin and lutein-zeaxanthin were

positively correlated with chlorine, medium and fine-sands, PPI and chl-*a* content, while negatively correlated with echinenone and canthaxanthin. In contrast, echinenone and canthaxanthin were positively correlated with OM, $\delta^{15}\text{N}$, the BIT index, coarse-sandy fractions and β -

Table 3
Pigments identified in the *P. oceanica* mat cores in this study as well as their taxonomic affinities.

| Pigment | Algal group(s) |
|--------------------|---|
| Alloxanthin | Cryptophytes |
| Diadinoxanthin | Dinoflagellates, diatoms, chrysophytes |
| Diatoxanthin | Diatoms, chrysophytes |
| Lutein- Zeaxanthin | Higher plants, chlorophytes, rhodophytes ^a , cyanobacteria |
| Echinenone | Total cyanobacteria |
| Canthaxanthin | Nostocales cyanobacteria |
| β -carotene | Total phototrophs |

^a In marine ecosystems, lutein-zeaxanthin also represents the Rhodophyta (Esteban et al., 2009).

Table 4
Factor loadings of the PCA_{pigments} ran to explore potential associations in the community of primary producers as recorded by fossil pigment concentrations. Numbers in bold indicate pigments with highest factor loadings. Numbers in bold italics indicate pigments with moderate factor loadings.

| | PC1 _{pigments} | PC2 _{pigments} |
|--------------------|-------------------------|-------------------------|
| Variance explained | 78% | 13% |
| Diadinoxanthin | 0.85 | −0.07 |
| Alloxanthin | 0.14 | −0.07 |
| Diatoxanthin | −0.18 | 0.55 |
| Lutein-zeaxanthin | −0.23 | 0.49 |
| Canthaxanthin | −0.21 | −0.29 |
| Echinenone | −0.37 | −0.59 |

Table 5

Factor loadings of the PCA_{environmental} ran to decipher relationships between marker pigment composition and explicative variables. Numbers in bold indicate variables with the highest factor loadings and in bold. Numbers in bold and italics indicate variables with moderate factor loadings. Explicative variables are the Branched and Isoprenoid Tetraether (BIT) index -an index of the relative abundance of terrestrial organic matter versus marine input in marine sediments (Hopmans et al., 2004)-, Total Solar Irradiance (TSI, Vieira et al., 2011), index of North Atlantic Oscillation (NAO, Hurrell, 2003; Trouet et al., 2009; Olsen et al., 2012), Northern-Hemisphere Temperature (NHT, Kobashi et al., 2013), grain-size distribution, content of organic matter (OM), XRF-measured elements (Fe, Si, Ti, K, Ca, S, Cl and Br), carbon and nitrogen stable isotopes, chl-*a* and β -carotenes, and a pigment preservation index (chl-*a*/pheophytin *a*).

| | PC1 _{environmental} | PC2 _{environmental} |
|-----------------------|------------------------------|------------------------------|
| Variance explained | 31% | 26% |
| Diadinoxanthin | -0.53 | -0.08 |
| Alloxanthin | -0.01 | 0.00 |
| Diatoxanthin | 0.08 | -0.10 |
| Lutein-zeaxanthin | 0.13 | -0.10 |
| Canthaxanthin | 0.11 | 0.13 |
| Echinenone | 0.22 | 0.14 |
| β -carotenes | 0.16 | 0.19 |
| chl- <i>a</i> | -0.16 | -0.19 |
| Mud | 0.00 | 0.06 |
| Fine sands | -0.02 | -0.17 |
| Medium sands | -0.01 | -0.18 |
| Coarse sands | 0.02 | 0.29 |
| Gravel | 0.00 | 0.00 |
| Si | -0.04 | -0.02 |
| S | -0.01 | 0.10 |
| Br | 0.00 | 0.08 |
| Cl | 0.00 | -0.32 |
| K | 0.03 | 0.07 |
| Ca | 0.03 | 0.10 |
| Ti | 0.00 | 0.00 |
| Fe | 0.00 | 0.00 |
| TSI | -0.35 | 0.11 |
| NAO | 0.01 | -0.06 |
| NHT | -0.59 | 0.16 |
| BIT | 0.06 | 0.36 |
| $\delta^{13}\text{C}$ | -0.23 | -0.05 |
| $\delta^{15}\text{N}$ | -0.02 | 0.37 |
| OM | -0.17 | 0.43 |
| Preservation index | -0.18 | -0.21 |

carotene, and negatively with diatoxanthin and lutein-zeaxanthin (Fig. 5A and Table 5).

Overall, PC1_{environmental} scores exhibited an increasing trend towards the present in most cores, in particular during the last 150–300 years (Fig. 5B). Temporal trends of PC2_{environmental} scores showed no clear nor common pattern among cores through time, although they did show the same difference among embayments as described for PC2_{pigments} (Fig. 5B).

3.4. Dinocyst records

Dinocysts concentrations were low in sediments from both bays. They were 1–2 orders of magnitude higher in EP05 than in SM25 (Fig. 6). All dinocysts identified were of autotrophic affinity. In both bays, dinocyst concentrations were composed predominately of *Spiniferites* spp. and *Lingulodinium machaerophorum*. *L. machaerophorum* is the cyst produced by the motile form *Lingulodinium polyedrum*, a species which inhabits estuaries and coastal bays worldwide, including the Mediterranean Sea (Lewis and Hallett, 1997; Penna et al., 2006). The most notable feature of the dinocyst records is the presence of a trend towards increasing concentrations during the last two centuries, particularly for *Spiniferites* spp., *L. machaerophorum*, *Operculodinium* spp., and for total dinocysts (Fig. 6). These trends were significant only for EP05, which is perhaps related to the larger amount of samples processed in EP05 compared to SM25.

GAMs were employed to test if the temporal changes in concentrations of dinoflagellate pigment diadinoxanthin (as PC1_{pigments} scores) were similar to those recorded for dinocysts (Fig. 7). Here the differences

between the GAM-fitted pigments and cyst trends were estimated only for the most recent 250 yrs., the period during which there was directional change in fossil abundance in EP05. Comparisons were conducted between PC1_{pigments} and total cyst concentrations (TC), as well as between PC1_{pigments} and cysts from *Lingulodinium machaerophorum* (LM) and *Spiniferites* spp. (SS). Confidence intervals not encompassing zero, are indicative of significant differences between the smoothed trends (Rose et al., 2012). In EP05 core, no difference was observed between trends in any metric of cyst abundance (TC, LM or SS) and PC1 scores during the last 250 years (Fig. 7). Therefore, we infer that the increasing recent trend in PC1_{pigment} and by inference the dinoflagellate biomarker diadinoxanthin mainly reflect changes in fossil concentrations of dinoflagellate cysts at least in the EP05 core (Figs. 6 and 7).

4. Discussion

4.1. Seagrass phototrophic community

The overall composition of sedimentary pigments from the mat cores was consistent with the expected assemblage of primary producers observed in *P. oceanica* meadows. In general, modern macroalgal species are characteristically composed mainly of calcareous Rhodophyta and non-calcified Ochrophyta, whereas microalgal epiphytes usually include diatoms, dinoflagellates and cyanobacteria in declining relative abundance (Piazzi et al., 2016; Agawin et al., 2017). Similarly, the modern phytoplankton assemblages are mainly composed of diatoms and dinoflagellates (Moncer et al., 2017), while the water column near Cabrera is known to harbour a great abundance of pico and nanoplankton, dinoflagellates, coccolithophorids and diatoms (Vives, 1993). We suggest that seagrass, possibly in association with rhodophytes, is the main source of the couplet lutein-zeaxanthin, as it is the most abundant carotenoid in live *P. oceanica* tissues (Casazza and Mazella, 2002).

4.2. Observed temporal and spatial patterns

Multivariate analysis of the cores revealed two main patterns of change in the fossil pigment assemblages. First, we recorded a temporal shift in the abundance of dinoflagellates and siliceous algae, which appears to reflect the influence of global climate change, particularly the inputs of energy as irradiance and heat (i.e., TSI and NHT). Second, our results showed clear spatial patterns in primary producers' community composition, seemingly related to embayment-specific local conditions (EP versus SM), and to the water depth gradient (SM gradient). Taken together, these patterns suggest that primary producers in seagrass meadows are influenced by a combination of global and local regulatory mechanisms.

4.2.1. The recent increase in dinoflagellates

Increased abundance of dinoflagellates and possibly siliceous taxa (as the carotenoid diadinoxanthin) was observed among all cores over the last 150–300 years (Figs. 4 and 5). Our results suggest that the carotenoid diadinoxanthin was more abundant during episodes of high solar irradiance (i.e., TSI), air temperature (i.e., NHT) and, to a lesser extent, ecosystem production (i.e., $\delta^{13}\text{C}$ and chl-*a*) according to PC1_{environmental} (Fig. 5A). Hence, changes in dinoflagellate abundance seem to be influenced by global climate variables - specifically the input of energy as irradiance and heat. Changes in pigment preservation may also partly explain these historical trends, as noted with the direction of the pigment preservation index vector (Fig. 5A). Post-depositional degradation may contribute to the decline in labile diadinoxanthin with increasing sediment age (PC1_{pigments} and PC1_{environmental}, Figs. 4B and 5B). However, analysis of resting cysts from dinoflagellates in cores EP05 and SM25 also showed an increase in dinoflagellate abundance over the same period, especially for *L. machaerophorum* and *Spiniferites* spp. in EP05 (Fig. 6). Dinocysts are composed of highly resistant

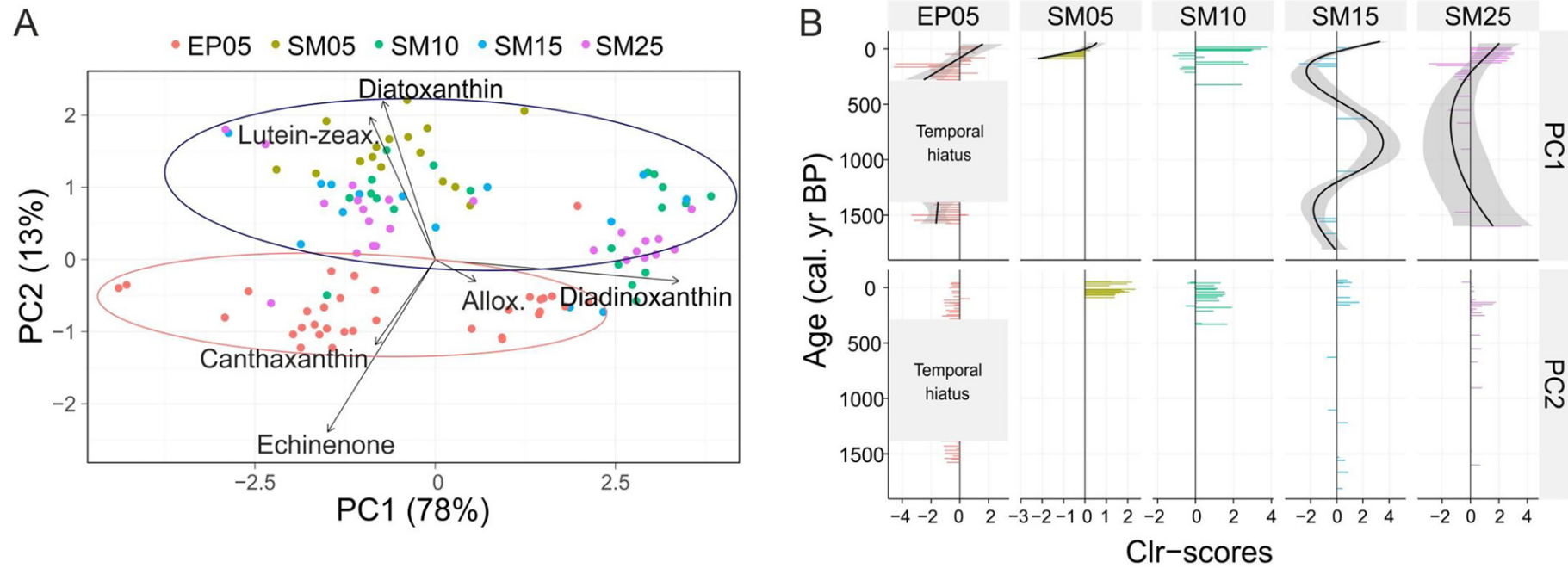


Fig. 4. $\text{PCA}_{\text{pigments}}$ run to explore potential associations in the community of primary producers as recorded by fossil pigment concentrations in the cores. **A)** Ckr-biplot of sample scores. Red ellipse indicates samples from EP and blue ellipse indicates samples from SM. **B)** Depth records of the $\text{PCA}_{\text{pigments}}$ scores. Black solid lines indicate fitted smooth functions of time (GAM models, formula = $y \sim s(x)$) and grey shaded regions are 95% point-wise confidence intervals. Only GAMs with significant trends are shown ($p > 0.05$). Algal groups associated to pigments are in Table 3.

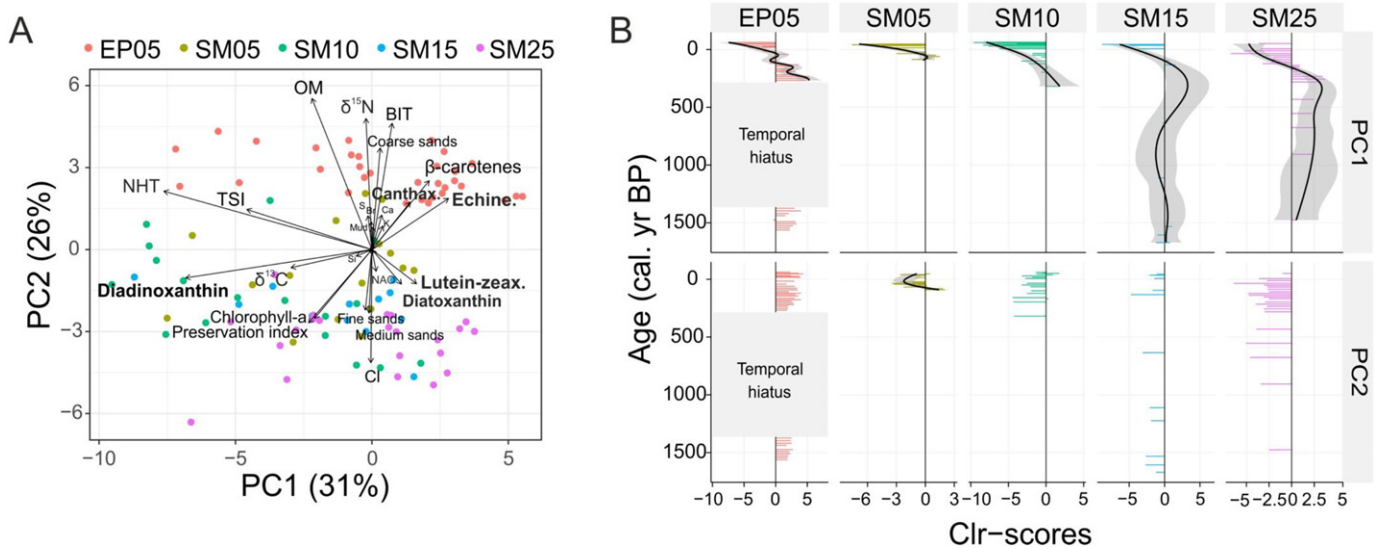


Fig. 5. PCA_{environmental} run to decipher relationships between fossil pigment composition and explicative variables: BIT index -an index of the relative abundance of terrestrial organic matter versus marine input in marine sediments (Hopmans et al., 2004), Total Solar Irradiance (TSI, Vieira et al., 2011), Index of North Atlantic Oscillation (NAO, Hurrell, 2003; Trouet et al., 2009; Olsen et al., 2012), Northern-Hemisphere Temperature (NHT, Kobashi et al., 2013), grain-size distribution, content of organic matter (OM), XRF-measured elements (Fe, Si, Ti, K, Ca, S, Cl and Br), carbon and nitrogen stable isotopes, chl-*a* and β -carotenes, and a pigment preservation index (chl-*a*/pheophytin *a*). **A)** CBr-biplot of sample scores. **B)** Depth records of the PC_{environmental} scores. Black solid lines indicate fitted smooth functions of time (GAM models, formula = $y \sim s(x)$) and grey shaded regions are 95% point-wise confidence intervals. Only GAMs with significant trends are shown ($p > 0.05$). Algal groups associated to pigments are in Table 3.

organic compounds, which are preserved well in sediments (Versteegh and Blokker, 2004). Given the strong concordance between historical trends in the dinoflagellate biomarker

diadinoxanthin (as PC1_{pigments}) and dinoflagellate cyst concentrations, we infer that increased abundance of diadinoxanthin over the past ~250 years reflects actual changes in algal biomass, rather

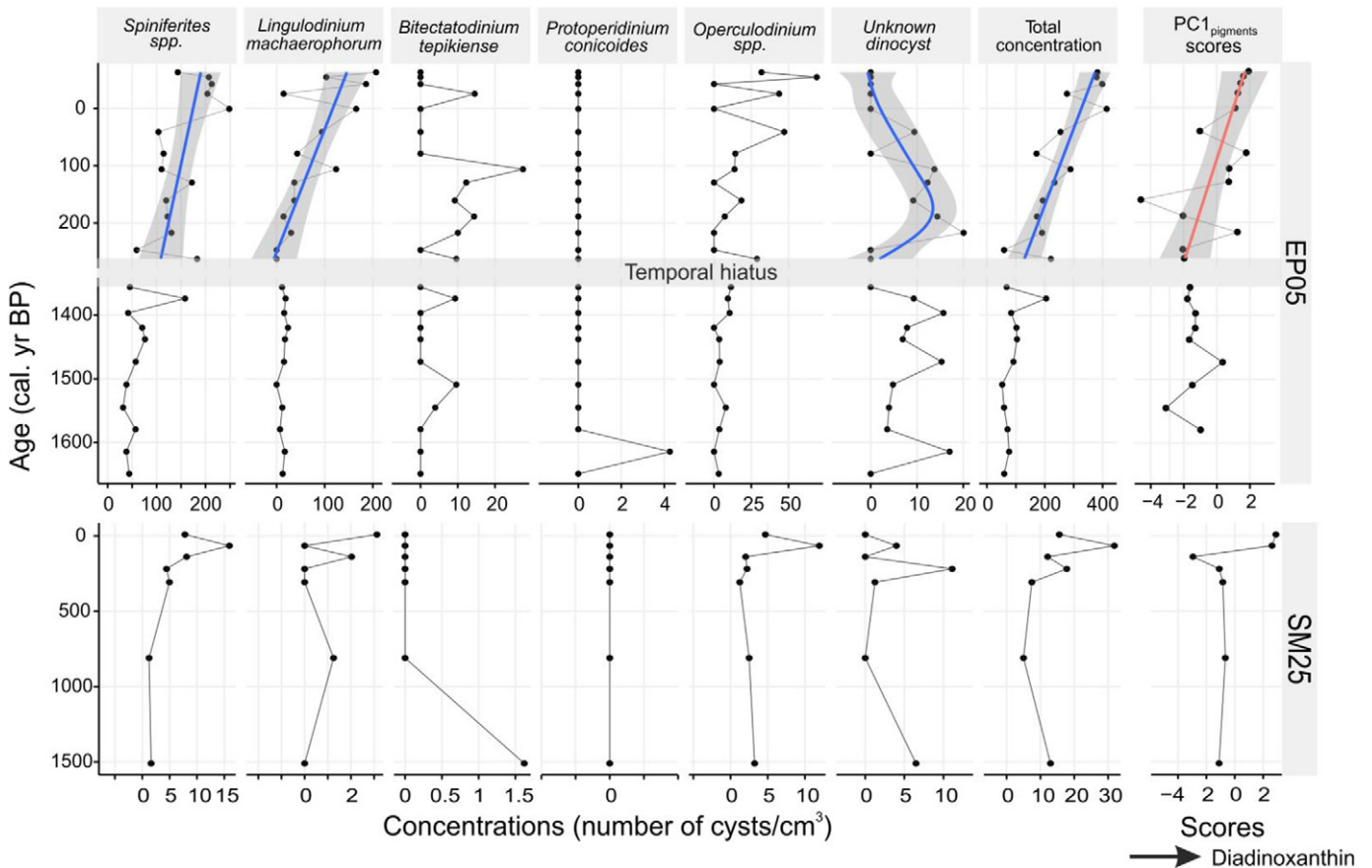


Fig. 6. Dinocyst concentrations records of cores EP05 and SM25 plotted together with PC1_{pigments} scores. Positive scores of PC1_{pigments} are related with higher concentrations of diadinoxanthin. Coloured solid lines indicate fitted smooth functions of time (GAM models, formula = $y \sim s(x)$) and grey shaded regions are 95% point-wise confidence intervals. Only GAMs with significant trends are shown ($p > 0.05$).

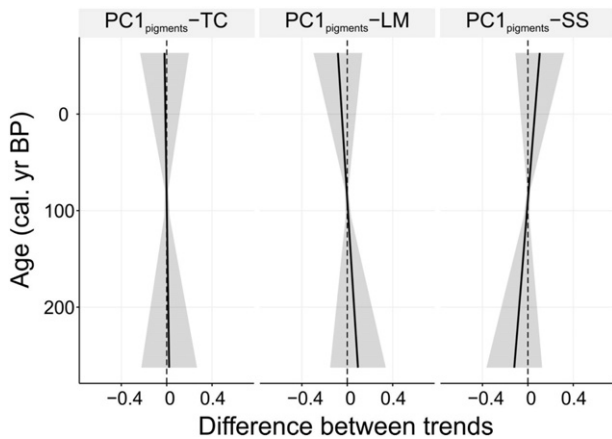


Fig. 7. Differences between fitted trends in the scores of $PC1_{\text{pigments}}$ and dinocysts records for the last 250 years in EP05. Black solid lines indicate differences between fitted smooth functions of time (GAM models, formula = $y \sim s(x)$) of $PC1_{\text{pigments}}$ scores, concentrations of total dinocysts (TC), *Lingulodinium machaerophorum* (LM) and *Spiniferites* spp. (SS). Grey shaded regions are 95% point-wise confidence intervals on these differences.

than slow post-depositional degradation in the *Posidonia* seagrass mats.

The observed orthogonal relationship between diadinoxanthin and diatoxanthin in the two PCAs was unexpected because both pigments usually co-occur in several algal groups, as in diatoms and dinoflagellates. Although speculative, this lack of correlation could be due to the fact that they are associated with different algal groups in the particular setting of Cabrera: diadinoxanthin with dinoflagellates and diatoxanthin with diatoms. Regardless, the uncorrelated nature of historical trends in diadinoxanthin and the diatom-specific biomarker diatoxanthin again suggests that historical trends in diadinoxanthin were recording mainly changes in marine dinoflagellate abundance.

Increased abundance of dinoflagellates during periods of elevated solar irradiance may be related to their ability to produce substantial amounts of UV-absorbing photo-protective compounds under high irradiance (Hannach and Sigleo, 1998). In this sense, diadinoxanthin is known to act as a photoprotective accessory pigment (Lavaud et al., 2002; Laviale and Jacques, 2011). Diadinoxanthin is not only present in dinoflagellates but also in some species of raphidophytes (e.g., *Heterosigma akashiwo*, *Chattonella subsalsa*), which also thrive in high UV environments (Fu et al., 2012; Wells et al., 2015). Similarly, elevated water temperature may favour growth of epiphytic dinoflagellates and diatoms in seagrass meadows (Johnson et al., 2005; Turki, 2005; Frankovich et al., 2006; Mabrouk et al., 2012). Moreover, the correlation between dinoflagellates and temperature found here was also described in several long-term dinocyst records, in which high *L. machaerophorum* and *Spiniferites* spp. abundance correlated with warmer sea surface waters and stronger stratified conditions in coastal areas (Pospelova et al., 2006; Sobrino et al., 2012; Bringué et al., 2013; Leroy et al., 2013). Those studies also reported sharp increases in *L. machaerophorum* over the last century, similar to the patterns observed in this study (Fig. 5A). *L. machaerophorum* is also a potentially-toxic taxon, known to produce yessotoxins (e.g. Paz et al., 2004; Armstrong and Kudela, 2006). Therefore, their higher abundance could increase the risk of toxic algal blooms that could affect the entire ecosystem composition and structure (Sellner et al., 2003).

Our results provide a predictive understanding of the response of phototrophic assemblages in seagrass meadows to global change. Specifically, we anticipate an increase in dinoflagellates as a consequence of global warming. The exact consequences of this change in the composition of primary producers are so far unknown. Our study points to a greater contribution of autotrophic dinoflagellates to autotrophic production in seagrass meadows, possibly leading to the outcompetition of the seagrass (Fig. 5A). Providing dinoflagellates do not outcompete

the seagrass and go through mass encystment, they could even have an effective contribution to carbon sequestration (Spilling et al., 2014; Wasmund et al., 2017). However, the latter speculation may be difficult to evaluate, as *P. oceanica* is thought to be negatively impacted by the on-going sea water warming (Marbà and Duarte, 2010; Savva et al., 2018).

4.2.2. Spatial differences between bays and along water depth

Our results revealed pronounced spatial patterns in primary producer community composition, caused by site-specific local effects, as well as the natural depth gradient. In the anthropogenically-impacted EP setting, the community was mainly dominated by cyanobacteria (as canthaxanthin and echinenone), whereas diatoms (as diatoxanthin), chlorophytes, rhodophytes and, most probably, the seagrass (all as lutein-zeaxanthin) were more characteristic of the less disturbed SM setting. As detailed below, these patterns may arise because of basin-specific differences in local land use and catchment characteristics, specifically nutrient and terrestrial organic matter inputs.

The cyanobacteria-rich community of EP developed in an environment with elevated organic matter and nutrient inputs, mainly of terrestrial origin (high loadings for BIT index, $\delta^{15}\text{N}$ and OM in $PC2_{\text{environmental}}$, Fig. 5). In EP, higher microbial decay would also explain the $\delta^{15}\text{N}$ enriched sediment organic matter relative to that of SM (Craine et al., 2015). Aside from high nutrient availability, EP waters have other physical conditions favourable to elevated cyanobacterial abundance compared to SM, such as longer water residence times and enhanced stratification (Orfila et al., 2005; Paerl and Huisman, 2008). On the other hand, diatoms, the seagrass and likely, rodophytes prevailed in SM (Fig. 4A), where organic matter is mainly derived from marine autochthonous production, as indicated by a high loading for chlorine in $PC2_{\text{environmental}}$ (Fig. 5A), an element known to be incorporated in labile marine organic matter (Leri et al., 2015). Our findings support those of Holmer et al. (2003, 2004) who reported an organic enrichment and higher mineralization rates in EP, as well as a significantly higher net community production in SM, reflecting higher light availability, lower terrestrial inputs and higher water turnover rates.

Studies of phytoplankton communities in marine waters have observed increases in the abundance of cyanobacteria under ammonium enrichment, whereas diatoms more commonly bloom when exposed to elevated nitrate concentrations (Berg et al., 2003; Heil et al., 2007; Glibert et al., 2014). Cyanobacteria are generally considered specialists that have a superior ammonium uptake kinetics (Blomqvist et al., 1994; Lindell and Post, 2001). Further, cyanobacteria can use organic matter as a nitrogen source in both lakes and marine ecosystems (e.g., Berman, 2001; Sakamoto & Bryant, 2001; Berg et al., 2003; Glibert et al., 2004; Donald et al., 2011). Therefore, the predominance of cyanobacteria in EP could reflect an elevated influx of ammonium or other N species as a result of the enhanced organic matter decomposition in this bay (Holmer et al., 2004; Pérez et al., 2007), or higher availability of dissolved organic matter. The naturally high organic matter accumulation in EP arises from discharges of the main pluvial network of the island (Rodríguez-Perea and Servera, 1993), and from the longer water residence time in EP, which, together, may favour particle sedimentation and a larger contribution of allochthonous organic matter to the bottom deposits. In fact, Mazarrasa et al. (2017) observed that allochthonous carbon accounted for more carbon in meadows from EP than in other Balearic meadows, including SM.

At SM shallowest station (SM05, Fig. 4A), pigment assemblages indicated dominance of diatoms (diatoxanthin), seagrasses, and rhodophytes (lutein-zeaxanthin) compared to the deeper stations. A greater abundance of diatoms in the shallowest areas could be related to the diatoms' feature of developing better in turbulent, well-mixed waters (Mabrouk et al., 2011). The greater abundance of seagrass at shallower depths could be explained by higher light availability and, therefore, higher photosynthetic rates and production (Alcoverro

et al., 2001). In general, water depth is a key regulator of epiphytes assemblages of seagrasses due to differences in the seagrass and meadow structural characteristics, light penetration, and hydrodynamics (Piazzi et al., 2016 and references therein).

5. Conclusions

The use of fossil pigments is feasible in sheltered vegetative coastal habitats. In this sense, this study pioneers in the use of fossil pigments in *P. oceanica* mats as proxy of phototrophs composition. Fossil pigments can be used in *Posidonia* spp. meadows, where chronologically ordered sequences are highly preserved in the sediments below them (i.e. the mats), but it could be also used in other smaller seagrass located in sheltered areas where sedimentation is not altered.

Our results report changes in phototrophic community composition and production in *P. oceanica* meadows at centennial scales. Analyses suggest that these changes were modulated by both local terrestrial influences and global climate factors. In particular, elevated solar irradiance and air temperature seem to have driven increases in dinoflagellates abundance over the last 150–300 years. Local environmental conditions were most likely responsible for differences in phototrophic communities between basins; apparently due to differences in terrestrial organic matter and nutrient inputs. Depth also influenced the phototrophic community composition, with greater predominance of pigments from diatoms, seagrasses and rodophytes in shallower waters.

These patterns confirm that primary producers in seagrass meadows are under complex hierarchical control by local and global regulatory mechanisms and provide better insights into potential phototrophic responses to global change. Specifically, we infer that global warming may favour the development of autotrophic dinoflagellate assemblages, which could negatively affect the ecosystem functioning by shading and outcompeting the seagrass. Future research could focus on the potential effects of these structural community changes on seagrass ecosystem functioning under predicted climate change scenarios.

Declaration of competing interest

The authors declare that they have no known competing financial interests or personal relationships that could have appeared to influence the work reported in this paper.

Acknowledgements

This research was supported by a PhD scholarship funded by the Spanish Ministry of Science, Innovation and Universities to C. Leiva-Dueñas (FPU15/01934); SUMILEN project (CTM2013-47728-R) funded by the Spanish Ministry of Economy and Competitiveness; and the PALEOPARK project funded by the Spanish Autonomous Organism of National Parks, (ref. 1104/2014). O. Serrano was supported by an ARC DECRA DE170101524. L. López-Merino was supported by a Leverhulme Early Career Fellowship (ECF-2013-530) for the palynological extraction at Brunel University London, and is currently performing the counting and palynological identifications thanks to PALAEOCON, a Marie Skłodowska-Curie Action (H2020-MSCA-IF-2018, Grant agreement ID: 833422) at the Universidade de Santiago de Compostela. Pigment analyses were supported by the Natural Sciences and Engineering Research Council of Canada (NSERC), the Canada Foundation for Innovation (CFI), and the Canada Research Chairs (CRC) programs, the Province of Saskatchewan, University of Regina and Queen's University Belfast. GDGT analysis was supported by the Netherlands Earth System Science Centre financed by the Dutch Ministry of Education and Science. We thank Deirdre Bateson for pigment analyses, Dr. Thomas Hoyle and Manuel Sala for their help in the identification of dinocysts, Karsten Dekker (NIOZ) for GDGT analysis as well as Nerea Piñeiro-Juncal, Anna Thoran and Ambra Milani for their involvement in field work and

laboratory analyses. This is a paper of the Group of Benthic Ecology 2014 SGR 120 of the Group of Aquatic Macrophyte Ecology (GAME).

Appendix A. Supplementary data

Supplementary data to this article can be found online at <https://doi.org/10.1016/j.scitotenv.2020.137163>.

References

- Agawin, N.S.R., Ferriol, P., Sintes, E., Moyà, G., 2017. Temporal and spatial variability of in situ nitrogen fixation activities associated with the Mediterranean seagrass *Posidonia oceanica* meadows. *Limnol. Oceanogr.* 62, 2575–2592. <https://doi.org/10.1002/lno.10591>.
- Aitchison, J., 1986. *The statistical analysis of compositional data*. Chapman & Hall, Ltd., London.
- Alcover, J.A., Ballesteros, E., Fornós, J.J., 1993. *Història natural de l'Arxipèlag de Cabrera*. MOLL-CSIC, Madrid.
- Alcoverro, T., Cebrian, E., Ballesteros, E., 2001. The photosynthetic capacity of the seagrass *Posidonia oceanica*: influence of nitrogen and light. *J. Exp. Mar. Bio. Ecol.* 261, 107–120. [https://doi.org/10.1016/S0022-0981\(01\)00267-2](https://doi.org/10.1016/S0022-0981(01)00267-2).
- Armitage, A.R., Frankovich, T.A., Fourqurean, J.W., 2006. Variable responses within epiphytic and benthic microalgal communities to nutrient enrichment. *Hydrobiologia* 569, 423–435. <https://doi.org/10.1007/s10750-006-0146-8>.
- Armstrong, M., Kudela, R., 2006. Evaluation of California isolates of *Lingulodinium polyedrum* for the production of yessotoxin. *African J. Mar. Sci.* 28. <https://doi.org/10.2989/18142320609504186>.
- Ballesteros, E., Zabala, M., 1993. El bentos: El marc físic. In: Alcover, J.A., Ballesteros, E., Fornós, J.J. (Eds.), *Història Natural de l'arxipèlag de Cabrera*. Moll. Monogr. Soc. Hist. Nat. Balears 2, Madrid, pp. 663–685.
- Berg, G.M., Balode, M., Purina, I., Purvina, S., Christian, B., Serge, M., 2003. Plankton community composition in relation to availability and uptake of oxidized and reduced nitrogen. *Aquat. Microb. Ecol. (Inter-research)* 30 (3), 263–274. <https://doi.org/10.3354/ame030263>.
- Berman, T., 2001. The role of DON and the effect of N:P ratios on occurrence of cyanobacterial blooms: implications from the outgrowth of *Aphanizomenon* in Lake Kinneret. *Limnol. Oceanogr.* - LIMNOL Ocean. 46, 443–447. <https://doi.org/10.4319/lno.2001.46.2.0443>.
- Blomqvist, P., Pettersson, A., Hyenstrand, P., 1994. Ammonium-nitrogen - a key regulatory factor causing dominance of non-nitrogen-fixing cyanobacteria in aquatic systems. *Arch. Fur Hydrobiol.* 132, 141–164.
- Borowitzka, M.A., Lavery, P.S., Keulen, M., 2006. Epiphytes of seagrasses. In: Larkum, A.W.D., Orth, R.J., Duarte, C.M. (Eds.), *Seagrasses: Biology, Ecology and Conservation*. Springer, Dordrecht, pp. 441–461.
- Boudouresque, C.F., Shili, A., Verlaque, M., Paoli, D.C.P., 2009. Regression of Mediterranean Seagrasses Caused by Natural Processes and Anthropogenic Disturbances and Stress: A Critical Review. vol. 52, pp. 395–418. <https://doi.org/10.1515/BOT.2009.057>.
- Bringué, M., Pospelova, V., Pak, D., 2013. Seasonal production of organic-walled dinoflagellate cysts in an upwelling system: a sediment trap study from the Santa Barbara Basin, California. *Mar. Micropaleontol.* 100, 34–51. <https://doi.org/10.1016/j.marmicro.2013.03.007>.
- Casazza, G., Mazella, L., 2002. Photosynthetic pigment composition of marine angiosperms: preliminary characterization of Mediterranean seagrasses. *Bull. Mar. Sci.* 71, 1171–1181.
- Craine, J.M., Brookshire, E.N.J., Cramer, M.D., Hasselquist, N.J., Koba, K., Mar, E., Wang, L., 2015. Ecological interpretations of nitrogen isotope ratios of terrestrial plants and soils. *Plant Soil* 396 (1), 1–26. <https://doi.org/10.1007/s11104-015-2542-1>.
- Delgado, O., Ruiz, J., Pérez, M., Romero, J., Ballesteros, E., 1999. Effects of fish farming on seagrass (*Posidonia oceanica*) in a Mediterranean bay: seagrass decline after organic loading cessation. *Oceanol. Acta* 22, 109–117. [https://doi.org/10.1016/S0399-1784\(99\)80037-1](https://doi.org/10.1016/S0399-1784(99)80037-1).
- Donald, D., Bogard, M., Finlay, K., Leavitt, P., 2011. Comparative effects of urea, ammonium, and nitrate on phytoplankton abundance, community composition, and toxicity in hypereutrophic freshwaters. *Limnol. Oceanogr.* 56, 2161. <https://doi.org/10.4319/lno.2011.56.6.2161>.
- Egozcue, J.J., Pawłowsky-Glahn, V., Mateu-Figueras, G., Barceló-Vidal, C., 2003. Isometric logratio transformations for compositional data analysis. *Math. Geol.* 35, 279–300. <https://doi.org/10.1023/A:1023818214614>.
- Fægri, K., Iversen, J., 1989. In: Fægri, K., Kaland, P.E., Krzywinski, K. (Eds.), *Textbook of pollen analysis*, 4th ed. John Wiley and Sons, Chichester (UK) (328 pp).
- Filzmoser, P., Hron, K., Reimann, C., 2010. The bivariate statistical analysis of environmental (compositional) data. *Sci. Total Environ.* 408, 4230–4238. <https://doi.org/10.1016/j.scitotenv.2010.05.011>.
- Frankovich, T., Gaiser, E., Ziemann, J., Wachnicka, A., 2006. Spatial and temporal distributions of epiphytic diatoms growing on *Thalassia testudinum* Banks ex König: relationships to water quality. *Hydrobiologia* 569, 259–271. <https://doi.org/10.1007/s10750-006-0136-x>.
- Fu, F.X., Tatters, A.O., Hutchins, D.A., 2012. Global change and the future of harmful algal blooms in the ocean. *Mar. Ecol. Prog. Ser.* 470, 207–233.
- Glibert, P., Heil, C., Hollander, D., Revilla, M., Hoare, A., Alexander, J., Murasko, S., 2004. Evidence for dissolved organic nitrogen and phosphorus uptake during a cyanobacterial bloom in Florida Bay. *Mar. Ecol. Prog. Ser.* 280, 73–83. <https://doi.org/10.3354/meps280073>.

- Glibert, P., Wilkerson, F., Dugdale, R., Parker, A., Alexander, J., Blaser, S., Murasko, S., 2014. Phytoplankton communities from San Francisco Bay Delta respond differently to oxidized and reduced nitrogen substrates— even under conditions that would otherwise suggest nitrogen sufficiency. *Front. Mar. Sci.* 1, 1–16. <https://doi.org/10.3389/fmars.2014.00017>.
- Hannach, G., Sigleo, A., 1998. Photoinduction of UV-absorbing compounds in six species of marine phytoplankton. *Mar. Ecol. Prog. Ser.* 174, 207–222. <https://doi.org/10.3354/meps174207>.
- Hay, W.W., 1974. Introduction. In: Hay, W.W. (Ed.), *Studies in Paleo-Oceanography*. SEPM Society for Sedimentary Geology. <https://doi.org/10.2110/pec.74.20>.
- Heil, C., Revilla, M., Glibert, P., Murasko, S., 2007. Nutrient quality drives phytoplankton community composition on the West Florida Shelf. *Limnol. Oceanogr.* 52, 1067–1078. <https://doi.org/10.4319/lo.2007.52.3.1067>.
- Hemminga, M.A., Duarte, C.M., 2000. *Seagrass Ecology*. Cambridge University Press <https://doi.org/10.1017/CBO9780511525551>.
- Holmer, M., Duarte, C.M., Marbà, N., 2003. Sulfur cycling and seagrass (*Posidonia oceanica*) status in carbonate sediments. *Biogeochemistry* 66, 223–239. <https://doi.org/10.1023/B:BIOG.0000005326.35071.51>.
- Holmer, M., Duarte, C., Boschker, H., Barrón, C., 2004. Carbon cycling and bacterial carbon sources in pristine and impacted Mediterranean seagrass sediments. *Aquat. Microb. Ecol.* 36, 227–237. <https://doi.org/10.3354/ame036227>.
- Holmer, M., Duarte, C.M., Marbà, N., 2005. Iron additions reduce sulfate reduction rates and improve seagrass growth on organic-enriched carbonate sediments. *Ecosystems* 8, 721–730. <https://doi.org/10.1007/s10021-003-0180-6>.
- Hopmans, E., Weijers, J., Schefuß, E., Herfort, L., Sinnighe-Damste, J., Schouten, S., 2004. A novel proxy for terrestrial organic matter in sediments based on branched and isoprenoid tetraether lipids. *Earth Planet. Sci. Lett.* 224, 107–116. <https://doi.org/10.1016/j.epsl.2004.05.012>.
- Hurrell, J., 2003. NAO Index Data provided by the Climate Analysis Section: “NAO Station Based (Annual)” [WWW Document]. Updat. Regul. URL <https://climatedataguide.ucar.edu/climate-data/hurrell-north-atlantic-oscillation-nao-index-station-based> (accessed 7.13.19).
- Johnson, M.P., Edwards, M., Bunker, F., Maggs, C.A., 2005. Algal epiphytes of *Zostera marina*: variation in assemblage structure from individual leaves to regional scale. *Aquat. Bot.* 82, 12–26. <https://doi.org/10.1016/j.aquabot.2005.02.003>.
- Kaal, J., Serrano, O., Nierop, K.G.J., Schellekens, J., Martínez-Cortizas, A., Mateo, M.A., 2016. Molecular composition of plant parts and sediment organic matter in a Mediterranean seagrass (*Posidonia oceanica*) mat. *Aquat. Bot.* 133, 50–61. <https://doi.org/10.1016/j.aquabot.2016.05.009>.
- Kobashi, T., Goto-Azuma, K., Box, J., Gao, C., Nakaegawa, T., 2013. Causes of Greenland temperature variability over the past 4000 yr: implications for northern hemispheric temperature changes. *Clim. Past* 9, 2299–2317. <https://doi.org/10.5194/cp-9-2299-2013>.
- Koch, E.W., 2001. Beyond light: physical, geological, and geochemical parameters as possible submersed aquatic vegetation habitat requirements. *Estuaries* 24, 1–17. <https://doi.org/10.2307/1352808>.
- Kowalewska, G., Wawrzyniak-Wydrowska, B., Szymczak-Zyła, M., 2004. Chlorophyll *a* and its derivatives in sediments of the Odra estuary as a measure of its eutrophication. *Mar. Pollut. Bull.* 49, 148–153. <https://doi.org/10.1016/j.marpolbul.2004.02.003>.
- Lavaud, J., Rousseau, B., van Gorkom, H., Etienne, A.-L., 2002. Influence of the diadinoxanthin pool size on photoprotection in the marine planktonic diatom *Phaeodactylum tricornutum*. *Plant Physiol.* 129, 1398–1406. <https://doi.org/10.1104/pp.002014>.
- Lavery, P.S., Reid, T., Hyndes, G.A., 2007. Effect of leaf movement on epiphytic algal biomass of seagrass leaves. *Mar. Ecol. Prog. Ser.* 338, 97–106.
- Laviale, M., Jacques, N., 2011. Relationships between pigment ratios and growth irradiance in 11 marine phytoplankton species. *Mar. Ecol. Prog. Ser.* 425, 63–77. <https://doi.org/10.3354/meps09013>.
- Leavitt, P., Hodgson, D., 2001. Sedimentary pigments. In: Smol, J.P., Birks, H.J.B., Last, W.M. (Eds.), *Tracking Environmental Changes Using Lake Sediments. Volume 3: Terrestrial, Algal, and Siliceous Indicators*. Kluwer Academic Publishers, Dordrecht, The Netherlands, pp. 295–325.
- Leiva-Dueñas, C., López-Merino, L., Serrano, O., Martínez Cortizas, A., Mateo, M.A., 2018. Millennial-scale trends and controls in *Posidonia oceanica* (L. Delile) ecosystem productivity. *Glob. Planet. Change* 169. <https://doi.org/10.1016/j.gloplacha.2018.07.011>.
- Leri, A.C., Mayer, L.M., Thornton, K.R., Northrup, P.A., Dunigan, M.R., Ness, K.J., Gellis, A.B., 2015. A marine sink for chlorine in natural organic matter. *Nat. Geosci.* 8, 620–624. <https://doi.org/10.1038/ngeo2481>.
- Leroy, S.A.G., Lahijani, H.A.K., Reyss, J.-L., Chalié, F., Haghani, S., Shah-Hosseini, M., Shahkarami, S., Tudryn, A., Arpe, K., Habibi, P., Nasrollahzadeh, H.S., Makhlough, A., 2013. A two-step expansion of the dinocyst *Lingulodinium machaerophorum* in the Caspian Sea: the role of changing environment. *Quat. Sci. Rev.* 77, 31–45. <https://doi.org/10.1016/j.quascirev.2013.06.026>.
- Lewis, J., Hallett, R., 1997. *Lingulodinium polyedrum* (Gonyaulax polyedra) a blooming dinoflagellate. *Oceanogr. Mar. Biol.* 35, 97–161.
- Lindell, D., Post, A.F., 2001. Ecological aspects of ntcA gene expression and its use as an indicator of the nitrogen status of marine *Synechococcus* spp. *Appl. Environ. Microbiol.* 67, 3340–3349. <https://doi.org/10.1128/AEM.67.8.3340-3349.2001>.
- Lo Iacono, C., Mateo, M.A., Gràcia, E., Guasch, L., Carbonell, R., Serrano, L., Serrano, O., Dañobeitia, J., 2008. Very high-resolution seismo-acoustic imaging of seagrass meadows (Mediterranean Sea): implications for carbon sink estimates. *Geophys. Res. Lett.* 35, L18601. <https://doi.org/10.1029/2008GL034773>.
- López-Merino, L., Serrano, O., Adame, M.F., Mateo, M.A., Martínez Cortizas, A., 2015. Glomalin accumulated in seagrass sediments reveals past alterations in soil quality due to land-use change. *Glob. Planet. Change* 133, 87–95. <https://doi.org/10.1016/j.gloplacha.2015.08.004>.
- López-Merino, L., Colás-Ruiz, N.R., Adame, M.F., Serrano, O., Martínez Cortizas, A., Mateo, M.A., 2017. A six thousand-year record of climate and land-use change from Mediterranean seagrass mats. *J. Ecol.* 105, 1267–1278. <https://doi.org/10.1111/1365-2745.12741>.
- López-Sáez, J.A., López-Merino, L., Mateo, M.A., Serrano, Ó., Pérez-Díaz, S., Serrano, L., 2009. Palaeoecological potential of the marine organic deposits of *Posidonia oceanica*: a case study in the NE Iberian Peninsula. *Palaeogeogr. Palaeoclimatol. Palaeoecol.* 271, 215–224. <https://doi.org/10.1016/j.palaeo.2008.10.020>.
- de los Santos, C.B., Krause-Jensen, D., Alcoverro, T., Marbà, N., Duarte, C.M., van Katwijk, M.M., Pérez, M., Romero, J., Sánchez-Lizaso, J.L., Roca, G., Jankowska, E., Pérez-Lloréns, J.L., Fournier, J., Montefalcone, M., Pergent, G., Ruiz, J.M., Cabaço, S., Cook, K., Wilkes, R.J., Moy, F.E., Trayter, G.M.-R., Arañó, X.S., de Jong, D.J., Fernández-Torquemada, Y., Auby, I., Vergara, J.J., Santos, R., 2019. Recent trend reversal for declining European seagrass meadows. *Nat. Commun.* 10, 3356. <https://doi.org/10.1038/s41467-019-11340-4>.
- Mabrouk, L., Hamza, A., Ibrahim, M. Ben, Bradai, M.-N., 2011. Temporal and depth distribution of microepiphytes on *Posidonia oceanica* (L.) Delile leaves in a meadow off Tunisia. *Mar. Ecol. Prog. Ser.* 32, 148–161. <https://doi.org/10.1111/j.1439-0485.2011.00432.x>.
- Mabrouk, L., Hamza, A., Mahfoudi, M., Bradai, M., 2012. Spatial and temporal variations of epiphytic *Ostreopsis siamensis* on *Posidonia oceanica* (L.) Delile leaves in Mahdia (Tunisia). *Cah. Biol. Mar.* 53, 419–427.
- Mabrouk, L., Ibrahim, M. Ben, Hamza, A., Bradai, M., 2014. Temporal and spatial zonation of macroepiphytes on *Posidonia oceanica* (L.) Delile leaves in a meadow off Mar. Ecol. 36, 77–92. <https://doi.org/10.1111/maec.12118>.
- Macreadie, P., Rolph, T., Boyd, R., Schroder-Adams, C., Skilbeck, C., 2015. Do ENSO and Coastal Development Enhance Coastal Burial of Terrestrial Carbon? *PLoS One* 10, e0145136. <https://doi.org/10.1371/journal.pone.0145136>.
- Marbà, N., Duarte, C., 2010. Mediterranean warming triggers seagrass (*Posidonia oceanica*) shoot mortality. *Glob. Chang. Biol.* 16, 2366–2375. <https://doi.org/10.1111/j.1365-2486.2009.02130.x>.
- Marbà, N., Duarte, C.M., Holmer, M., Martínez, R., Basterretxea, G., Orfila, A., Jordi, A., Tintoré, J., 2002. Effectiveness of protection of seagrass (*Posidonia oceanica*) populations in Cabrera National Park (Spain). *Environ. Conserv.* 29, 509–518. <https://doi.org/10.1017/S037689290200036X>.
- Marbà, N., Duarte, C.M., Holmer, M., Calleja, M.L., Álvarez, E., Díaz-Almela, E., Garcías-Bonet, N., 2008. Sedimentary iron inputs stimulate seagrass (*Posidonia oceanica*) population growth in carbonate sediments. *Estuar. Coast. Shelf Sci.* 76, 710–713. <https://doi.org/10.1016/j.ecss.2007.07.021>.
- Marbà, N., Arias-Ortiz, A., Masqué, P., Kendrick, G., Mazarrasa, I., Bastyan, G., García-Orellana, J., Duarte, C., 2015. Impact of seagrass loss and subsequent revegetation on carbon sequestration and stocks. *J. Ecol.* 103, 296–302. <https://doi.org/10.1111/1365-2745.12370>.
- Mateo, M.A., Romero, J., Pérez, M., Littler, M.M., Littler, D.S., 1997. Dynamics of millenary organic deposits resulting from the growth of the Mediterranean seagrass *Posidonia oceanica*. *Estuar. Coast. Shelf Sci.* 44, 103–110.
- Mateo, M.A., Cebrián, J., Dunton, K., Mutchler, T., 2006. Carbon flux in seagrass ecosystems. *Biol. Ecol. Conserv.* 159–192.
- Mateo, M.A., Renom, P., Michener, R.H., 2010. Long-term stability in the production of a NW Mediterranean *Posidonia oceanica* (L.) Delile meadow. *Palaeogeogr. Palaeoclimatol. Palaeoecol.* 291, 286–296. <https://doi.org/10.1016/j.palaeo.2010.03.001>.
- Mazarrasa, I., Marbà, N., García-Orellana, J., Masqué, P., Arias-Ortiz, A., Duarte, C., 2017. Dynamics of carbon sources supporting burial in seagrass sediments under increasing anthropogenic pressure. *Limnol. Oceanogr.* 62, 1451–1465. <https://doi.org/10.1002/lno.10509>.
- McGlathery, K., Sundbäck, K., Anderson, I., 2007. Eutrophication in shallow coastal bays and lagoons: the role of plants in the coastal filter. *Mar. Ecol. Prog. Ser.* 348, 1–18.
- McRoy, C., McMillan, C., 1977. Production ecology and physiology of seagrasses. In: McRoy, C., Helfferich, C. (Eds.), *Seagrass Ecosystems: A Scientific Perspective*. Dekker, New York, pp. 53–81.
- Moncer, M., Hamza, A., Feki, W., Mabrouk, L., Hassen, M., 2017. Variability patterns of epibenthic microalgae in eastern Tunisian coasts. *Sci. Mar.* 81, 487–498. <https://doi.org/10.3989/scimar.04651.17A>.
- Morton, R.A., White, W.A., 1997. Characteristics of and corrections for core shortening in unconsolidated sediments. *J. Coast. Res.* 13, 761–769.
- Nesti, U., Piazzi, L., Balata, D., 2009. Variability in the structure of epiphytic assemblages of the Mediterranean seagrass *Posidonia oceanica* in relation to depth. *Mar. Ecol. Prog. Ser.* 30, 276–287. <https://doi.org/10.1111/j.1439-0485.2008.00275.x>.
- Olsen, J., Anderson, N.J., Knudsen, M.F., 2012. Variability of the North Atlantic oscillation over the past 5,200 years. *Nat. Geosci.* 5, 808–812. <https://doi.org/10.1038/ngeo1589>.
- Orfila, M., Hernández, M., Cau Ontiveros, M., 1992. Nuevos datos sobre el poblamiento antiguo de la isla de Cabrera (Balears): Una posible factoría de salazones. *Sagvntum*, p. 25. <https://doi.org/10.7203/SAGVNTUM.3644>.
- Orfila, A., Jordi, A., Basterretxea, G., Vizoso, G., Marbà, N., Duarte, C., Werner, F.E., Tintoré, J., 2005. Residence time and *Posidonia oceanica* in Cabrera Archipelago National Park, Spain. *Cont. Shelf Res.* 25, 1339–1352. <https://doi.org/10.1016/j.csr.2005.01.004>.
- Paeli, H., Huisman, J., 2008. Blooms Like It Hot. *Science* 320, 57–58. <https://doi.org/10.1126/science.1155398>.
- Paz, B., Riobó, P., Fernández, M.L., Fraga, S., Franco, J.M., 2004. Production and release of yessotoxins by the dinoflagellates *Protoceratium reticulatum* and *Lingulodinium polyedrum* in culture. *Toxicol. Appl. Pharmacol.* 44, 251–258. <https://doi.org/10.1016/j.toxicol.2004.05.021>.
- Penna, A., Bertozzini, E., Battocchi, C., Galluzzi, L., Giacobbe, M.G., Vila, M., Garces, E., Lugliè, A., Magnani, M., 2006. Monitoring of HAB species in the Mediterranean Sea through molecular methods. *J. Plankton Res.* 29, 19–38. <https://doi.org/10.1093/plankt/fbi053>.

- Pérez, M., Invers, O., Ruiz Fernández, J.M., Frederiksen, M., Holmer, M., 2007. Physiological responses of the seagrass *Posidonia oceanica* to elevated organic matter content in sediments: an experimental assessment. *J. Exp. Mar. Bio. Ecol.* 344, 149–160. <https://doi.org/10.1016/j.jembe.2006.12.020>.
- Piazza, L., Balata, D., Ceccherelli, G., 2016. Epiphyte assemblages of the Mediterranean seagrass *Posidonia oceanica*: an overview. *Mar. Ecol.* 37, 3–41. <https://doi.org/10.1111/maec.12331>.
- Piñeiro Juncal, N., Mateo, M.Á., Holmer, M., Martínez-Cortizas, A., 2018. Potential microbial functional activity along a *Posidonia oceanica* soil profile. *Aquat. Microb. Ecol.* 81. <https://doi.org/10.3354/ame01872>.
- Pospelova, V., Pedersen, T., Anne, de V., 2006. Dinoflagellate cysts as indicators of climatic and oceanographic changes during the past 40 kyr in the Santa Barbara Basin, Southern California. *Paleoceanography* 21. <https://doi.org/10.1029/2005PA001251>.
- Prado, P., Alcoverro, T., Martínez-Crego, B., Vergés, A., Pérez, M., Romero, J., 2007. Macrograzers strongly influence patterns of epiphytic assemblages in seagrass meadows. *J. Exp. Mar. Bio. Ecol.* 350, 130–143. <https://doi.org/10.1016/j.jembe.2007.05.033>.
- R Core Team, 2018. *R: A Language and Environment for Statistical Computing*.
- Rabalais, N.N., Atilla, N., Normandeau, C., Turner, R.E., 2004. Ecosystem history of Mississippi River-influenced continental shelf revealed through preserved phytoplankton pigments. *Mar. Pollut. Bull.* 49, 537–547. <https://doi.org/10.1016/j.marpolbul.2004.03.017>.
- Ralph, P., Tomasko, D., Moore, K., Seddon, S., Macinnis-Ng, C., 2006. Human impacts on seagrasses: eutrophication, sedimentation and contamination. In: Larkum, A.W.D., Orth, R.J., Duarte, C.M. (Eds.), *Seagrasses: Biology, Ecology and Conservation*. Springer, Dordrecht, pp. 567–593.
- Reimer, P.J., Bard, E., Bayliss, A., Beck, J.W., Blackwell, P.G., Ramsey, C.B., Buck, C.E., Cheng, H., Edwards, R.L., Friedrich, M., Grootes, P.M., Guilderson, T.P., Hafflidason, H., Hajdas, I., Hatté, C., Heaton, T.J., Hoffmann, D.L., Hogg, A.G., Hughen, K.A., Kaiser, K.F., Kromer, B., Manning, S.W., Niu, M., Reimer, R.W., Richards, D.A., Scott, E.M., Southon, J.R., Staff, R.A., Turney, C.S.M., van der Plicht, J., 2013. IntCal13 and Marine13 radiocarbon age calibration curves 0–50,000 Years cal BP. *Radiocarbon* 55, 1869–1887. https://doi.org/10.2458/azu_js_rc.55.16947.
- Reuss, N., Conley, D.J., Bianchi, T.S., 2005. Preservation conditions and the use of sediment pigments as a tool for recent ecological reconstruction in four Northern European estuaries. *Mar. Chem.* 95, 283–302. <https://doi.org/10.1016/j.marchem.2004.10.002>.
- Reuss, N., Leavitt, R.L., Hall, R.J., Bigler, C., Hammarlund, D., 2010. Development and application of sedimentary pigments for assessing effects of climatic and environmental changes on subarctic lakes in northern Sweden. *J. Paleolimnol.* 43, 149–169. <https://doi.org/10.1007/s10933-009-9323-x>.
- Riera Rullan, M., 2016. *Arqueologia d'una Instal·lació Monacal Primerenca a l'Arxipèlag de Cabrera (Illes Balears) (Segles V–VIII DC) Restes Arquitectòniques de Producció, Ceràmica i Altres Materials Arqueològics*. Universitat Autònoma de Barcelona.
- Roberts, N., Moreno, A., Valero-Garcés, B.L., Corella, J.P., Jones, M., Allcock, S., Woodbridge, J., Morellón, M., Luterbacher, J., Xoplaki, E., Türkeş, M., 2012. Palaeolimnological evidence for an east–west climate see-saw in the Mediterranean since AD 900. *Glob. Planet. Change* 84–85, 23–34. <https://doi.org/10.1016/j.gloplacha.2011.11.002>.
- Rodríguez-Perea, A., Servera, J., 1993. *Geomorfologia*. In: Alcover, J., Ballesteros, E., Fornós, J. (Eds.), *Història Natural de l'arxipèlag de Cabrera*. Moll. Monogr. Soc. Hist. Nat. Balears 2, Madrid, pp. 33–60.
- Rose, N.L., Yang, H., Turner, S.D., Simpson, G.L., 2012. An assessment of the mechanisms for the transfer of lead and mercury from atmospherically contaminated organic soils to lake sediments with particular reference to Scotland, UK. *Geochim. Cosmochim. Acta* 82, 113–135. <https://doi.org/10.1016/j.gca.2010.12.026>.
- Savva, I., Bennett, S., Roca, G., Jordà, G., Marba, N., 2018. Thermal tolerance of Mediterranean marine macrophytes: vulnerability to global warming. *Ecol. Evol.* 8. <https://doi.org/10.1002/ece3.4663>.
- Schouten, S., Huguier, C., Hopmans, E.C., Kienhuis, M.V.M., Sinninghe Damsté, J.S., 2007. Analytical methodology for TEX86 paleothermometry by high-performance liquid chromatography/atmospheric pressure chemical ionization-mass spectrometry. *Anal. Chem.* 79, 2940–2944. <https://doi.org/10.1021/ac062339v>.
- Sellner, K.G., Doucette, G.J., Kirkpatrick, G.J., 2003. Harmful algal blooms: causes, impacts and detection. *J. Ind. Microbiol. Biotechnol.* 30, 383–406. <https://doi.org/10.1007/s10295-003-0074-9>.
- Serrano, O., Mateo, M.A., Dueñas-Bohórquez, A., Renom, P., López-Sáez, J.A., Martínez Cortizas, A., 2011. The *Posidonia oceanica* marine sedimentary record: a Holocene archive of heavy metal pollution. *Sci. Total Environ.* 409, 4831–4840. <https://doi.org/10.1016/j.scitotenv.2011.08.001>.
- Serrano, O., Mateo, M.A., Renom, P., Julià, R., 2012. Characterization of soils beneath a *Posidonia oceanica* meadow. *Geoderma* 185, 26–36. <https://doi.org/10.1016/j.geoderma.2012.03.020>.
- Serrano, O., Martínez-Cortizas, A., Mateo, M.A., Biester, H., Bindler, R., 2013. Millennial scale impact on the marine biogeochemical cycle of mercury from early mining on the Iberian Peninsula. *Glob. Biogeochem. Cycles* 27, 21–30. <https://doi.org/10.1029/2012GB004296>.
- Serrano, O., Lavery, P.S., López-Merino, L., Ballesteros, E., Mateo, M.A., 2016a. Location and associated carbon storage of erosional escarpments of seagrass *Posidonia* Mats. *Front. Mar. Sci.* 3, 42. <https://doi.org/10.3389/fmars.2016.00042>.
- Serrano, O., Davis, G., Lavery, P.S., Duarte, C.M., Martínez-cortizas, A., Angel, M., Masqué, P., Arias-Ortiz, A., Rozaimi, M., Kendrick, G.A., 2016b. Reconstruction of centennial-scale fluxes of chemical elements in the Australian coastal environment using seagrass archives. *Sci. Total Environ.* 541, 883–894. <https://doi.org/10.1016/j.scitotenv.2015.09.017>.
- Serrano, O., Lavery, P., Masque, P., Inostroza, K., Bongiovanni, J., Duarte, C., 2016c. Seagrass sediments reveal the long-term deterioration of an estuarine ecosystem. *Glob. Chang. Biol.* 22, 1523–1531. <https://doi.org/10.1111/gcb.13195>.
- Simpson, G.L., 2018. Modelling palaeoecological time series using generalised additive models. *Front. Ecol. Evol.* 6, 149. <https://doi.org/10.3389/fevo.2018.00149>.
- Sobrinho, C., García-Gil, S., Iglesias, J., Carreño, N., da Costa, J., Díaz Varela, R., Judd, A., 2012. Environmental change in the Ria de Vigo, NW Iberia, since the mid-Holocene: new palaeoecological and seismic evidence. *Boreas* 41, 578–601. <https://doi.org/10.1111/j.1502-3885.2012.00255.x>.
- Spalding, M., Taylor, M., Ravilious, C., Short, F., Green, E., 2003. *Global overview: the distribution and status of seagrasses*. In: Green, E.P., Short, F.T. (Eds.), *World Atlas of Seagrasses: Present Status and Future Conservation*. University of California Press, Berkeley, pp. 5–26.
- Spilling, K., Kremp, A., Klais, R., Olli, K., Tamminen, T., 2014. Spring bloom community change modifies carbon pathways and C:N:P: Chla stoichiometry of coastal material fluxes. *Biogeosciences* 11, 7275–7289. <https://doi.org/10.5194/bg-11-7275-2014>.
- Templ, M., Hron, K., Filzmoser, P., 2011. *robCompositions: an R-package for robust statistical analysis of compositional data*. In: Pawlowsky-Glahn, V., Buccianti, A. (Eds.), *Compositional Data Analysis: Theory and Applications*. John Wiley and Sons, Chichester (UK), pp. 341–355.
- Trouet, V., Esper, J., Graham, N., Baker, A., Scourse, J., Frank, D., 2009. Persistent positive North Atlantic oscillation mode dominated the medieval climate anomaly. *Science* 324, 78–80. <https://doi.org/10.1126/science.1166349>.
- Tsirika, A., Skoufas, G., Haritonidis, S., 2007. Seasonal and bathymetric variations of epiphytic macroflora on *Posidonia oceanica* (L.) Delile leaves in the National Marine Park of Zakynthos (Greece). *Mar. Ecol.* 28, 146–153. <https://doi.org/10.1111/j.1439-0485.2007.00170.x>.
- Turki, S., 2005. Distribution of toxic dinoflagellates along the leaves of seagrass *Posidonia oceanica* and *Cymodocea nodosa* from the Gulf of Tunis. *Cah. Biol. Mar.* 46, 29–34.
- Versteegh, G., Blokker, P., 2004. Resistant macromolecules of extant and fossil microalgae. *Phycol. Res.* 52, 325–339. <https://doi.org/10.1111/j.1440-183.2004.00361.x>.
- Viaroli, P., Bartoli, M., Giordani, G., Naldi, M., Orfanidis, S., Zaldivar, J.M., 2008. Community shifts, alternative stable states, biogeochemical controls and feedbacks in eutrophic coastal lagoons: a brief overview. *Aquat. Conserv. Mar. Freshw. Ecosyst.* 18, S105–S117. <https://doi.org/10.1002/aqc.956>.
- Vieira, L., Solanki, S., Krivova, N., Usoskin, I., 2011. Evolution of the solar irradiance during the Holocene. *Astron. Astrophys.* 531. <https://doi.org/10.1051/0004-6361/201015843>.
- Vives, F., 1993. *Aspectes Hidrogràfics i Planctònics dels Voltants de l'Arxipèlag de Cabrera*. In: Alcover, J.A., Ballesteros, E., Fornós, J.J. (Eds.), *Història Natural de l'arxipèlag de Cabrera*. Moll. Monogr. Soc. Hist. Nat. Balears 2, Madrid, pp. 487–502.
- Wasmund, N., Kownacka, J., Göbel, J., Jaanus, A., Johansen, M., Jurgensone, I., Lehtinen, S., Powilleit, M., 2017. The diatom/dinoflagellate index as an indicator of ecosystem changes in the Baltic Sea 1. Principle and handling instruction. *Front. Mar. Sci.* 4. <https://doi.org/10.3389/fmars.2017.00022>.
- Wells, M.L., Trainer, V.L., Smayda, T.J., Karlson, B.S.O., Trick, C.G., Kudela, R.M., Ishikawa, A., Bernard, S., Wulff, A., Anderson, D.M., Cochlan, W.P., 2015. Harmful algal blooms and climate change: learning from the past and present to forecast the future. *Harmful Algae* 49, 68–93. <https://doi.org/10.1016/j.hal.2015.07.009>.
- Wood, S.N., 2003. Thin plate regression splines. *J. R. Stat. Soc. Ser. B* 65, 95–114.
- Wood, S.N., 2004. Stable and efficient multiple smoothing parameter estimation for generalized additive models. *J. Am. Stat. Assoc.* 99, 673–686.
- Wood, S.N., 2017. *Generalized Additive Models: An Introduction with R*. 2nd ed. Chapman and Hall/CRC.
- Wood, S.N., Pya, N., Säfken, B., 2016. Smoothing parameter and model selection for general smooth models (with discussion). *J. Am. Stat. Assoc.* 111, 1548–1575.